China Geology 7 (2024) 586−588

China Geology

Journal homepage: http://chinageology.cgs.cn
https://www.sciencedirect.com/journal/china-geology

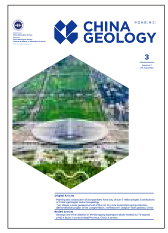

Short Communications (Research Advances)

Discovery of scheelite in the Zaozigou gold deposit of West Qinling Orogen, Northwest China and its implications for ore genesis

Meng-xu Guo[a], Jia-jun Liu[a,*], De-gao Zhai[a], Guo-ming Weng[a], Rui Zhu[b]

[a] *State Key Laboratory of Geological Processes and Mineral Resources, School of Earth Sciences and Resources, China University of Geosciences (Beijing), Beijing* 100083, *China*

[b] *Zaozigou Gold Mine, Zhaojin Mining Industry Co. Ltd., Hezuo* 747000, *China*

1. Objective

The West Qinling Orogen extends east-west over 1500 km and is endowed with dozens of large-super large scale gold deposits. The Zaozigou gold deposit has a proven reserve of 134 t with an average grade of 3.08 g/t thus is one of the largest deposits in the West Qinling Orogen. However, whether the fluid type is metamorphic or magmatic-hydrothermal and ore-formation processes of the Zaozigou gold deposit are equivocal. Scheelite is a ubiquitous accessory mineral in geologically diverse ore-deposit types and attested to be a strong indicator of ore-forming conditions and ore-deposit genesis. In this study, certain quantities of scheelite ($CaWO_4$) are documented for the first time in the Zaozigou gold deposit based on detailed hand specimens and microscopic observations, and mineralogical and trace-elemental characteristics of scheelite have been reported. The new discovery provides researchers with a tool to better understand the ore genesis of the Zaozigou gold deposit, contributing to further investigations into gold exploration in West Qinling Orogen.

2. Methods

The samples were collected from Line 83 of SD ZK 8314 drill hole (depth of 2001.5 m) in the the Zaozigou gold deposit at depths ranging from 361 m to 1995 m, then they were placed under an ultraviolet prospecting lamp to detect the presence of scheelite. Three scheelite-bearing samples (zzg-22, 48 and 62) were selected for polishing, microscopic and cathodoluminescence (CL) imaging and analysis of trace elements. Sample zzg-22, sampled in the depth interval from 1355 m to 1360 m, occurs as a quartz-scheelite vein (width of 1 cm to 2 cm) within quartz diorite with few stibnite grains (Fig. 1a). Sample zzg-48 occurs as quartz-calcite-scheelite vein (width of 3 cm to 4 cm) intersecting siliceous slate in the depth interval from 597 m to 598 m (Fig. 1b). Sample zzg-62 occurs as quartz-stibnite-scheelite vein (width of 1 cm to 2 cm) within quartz diorite porphyry with slight pyritization and sampled in the depth interval from 418 m to 431 m (Fig. 1c). Scheelite CL images were generated using a MK-CL-5200 with a Nikon Ds-Fi3 camera system. All measurements were performed at an accelerating voltage of 13 kV to 15 kV and a beam current of 250 μA. *In situ* LA-ICP-MS trace element analysis of scheelite was obtained using an East Laser LSPC-193-SS laser ablation system connected to a Jena PQ-MS Elite ICP-MS. The reference material NIST 610 was used as an external standard. NIST 612 was used as the unknown sample. Raw data reduction was carried out offline with Agilent 7500a workstation and Glitter 4.4.4. All observations and analyses were carried out in China University of Geosciences (Beijing).

3. Results

Scheelite-bearing samples were found in Zaozigou gold deposit. Scheelite appears bluish white to bluish grey under ultraviolet light and light grey to dark grey under reflected plane-polarized light (Figs. 1a–e). The photomicrographs show that scheelite occurs as individual grains with clusters up to 0.5 mm in size. Quartz and scheelite are intersected, filled or replaced by stibnite with some scheelite grains surrounded by calcite (Figs. 1d–e), indicating that quartz and scheelite formed earlier than stibnite and calcite. Visible gold occurs as inclusion gold enclosed in stibnite or fracture gold filling the fissures of quartz within quartz-stibnite-scheelite

First author: *E-mail address*: 1476895963@qq.com (Guo Meng-xu).

* Corresponding author: *E-mail address*: liujiajun@cugb.edu.cn (Jia-jun Liu).

Literary editor: Xi-jie Chen
doi:10.31035/cg2023099
2096-5192/© 2024 China Geology Editorial Office.

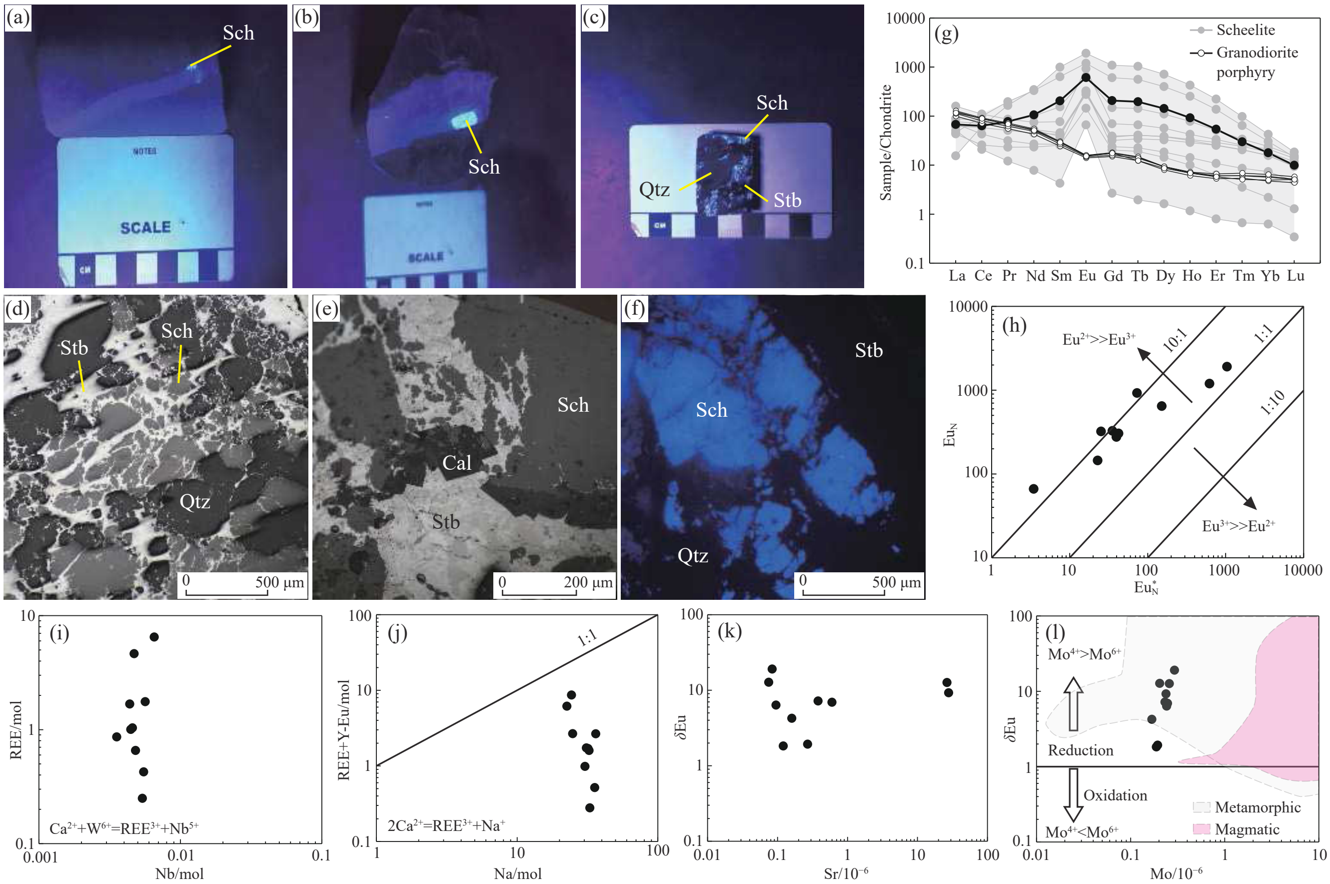

Fig. 1. Photographs of scheelite and plots showing variations of trace elements of scheelite from the Zaozigou gold deposit. a–c–hand-specimen photographs showing the occurrence of scheelite from ore samples zzg-22 (a), zzg-48 (b) and zzg-62 (c) under ultraviolet light. d–e–photomicrographs showing mineral assemblage containing scheelite, stibnite, quartz and calcite and mineralogical relationships. f–representative CL showing homogeneous scheelite. g–chondrite-normalized REE fractionation patterns of scheelite and granodiorite porphyry from the Zaozigou gold deposit. h–plot of chondrite-normalized Eu concentrations (Eu_N) *vs* calculated Eu_N^* values, where $Eu_N^* = (Sm_N \times Gd_N)^{1/2}$. Diagonal dashed lines show Eu_N / Eu_N^* ratios of 10,1 and 0.1. High Eu_N / Eu_N^* ratios indicate reduced fluid. i–j–binary diagrams of the mole fraction of REE *vs* Nb (i) and REE+Y−Eu *vs* Na (j). k–l–binary plots of δEu (δEu = Eu_N/ Eu_N^*) *vs* Sr (k) and δEu *vs* Mo (l). Cal–calcite, Qtz –quartz, Sch–scheelite, Stb–stibnite.

vein. Considering the intimate relations of scheelite, gold, stibnite and quartz, scheelite can thus provide clues for a better understanding of the Au mineralization. Under CL imaging, scheelite displays commonly homogeneous and lacks discernible zonation (Fig. 1f), which is analogous to scheelite formed in metamorphic environments.

Trace elements of scheelite from sample zzg-62 were examined by LA-ICP-MS (Table 1). The compositions of trace element of scheelite were illustrated in Figs. 1g–l. The chondrite-normalized REE patterns are MREE-enriched and slightly flat (LREE/HREE = 0.6 to 5.6) with an average Eu anomaly ($\delta Eu = Eu_N/Eu_N^*$, $Eu_N^* = (Sm_N \times Gd_N)^{1/2}$) of 8.22. In contrast, REE patterns of quartz diorite porphyry from the Zaozigou gold deposit are LREE-enriched (LREE/HREE = 5.5 to 6.5) with negative Eu anomalies (0.68 to 0.84) (Fig. 1g). The difference indicates the genetic fluid is unlikely related to the quartz diorite porphyry. The positive Eu anomalies of scheelite are influenced by pH, temperature and oxidation state of the ore-forming fluid (Figs. 1h, l). Binary plots of the mole fraction of REE against Nb (Fig. 1i) and REE+Y−Eu against Na (Fig. 1j) show no correlations, indicating the absence of substitutions $Ca^{2+} + W^{6+} = REE^{3+} + Nb^{5+}$ and $2Ca^{2+} = REE^{3+} + Na^+$, thus $3Ca^{2+} = 2REE^{3+} + \square Ca$ (where □Ca represents a Ca-site vacancy) can be the dominant substitution mechanism. Strontium and molybdenum in scheelite range from 0.08×10^{-6} to 26.44×10^{-6} (Fig. 1k) and 0.17×10^{-6} to 0.30×10^{-6} (Fig. 1l), respectively. The relative depletion in Sr could be due to early crystallization of plagioclase in magmatic settings, while low Mo contents may suggest reduced and metamorphic environments. In summary, the trace elemental characteristics of scheelite likely suggest a mixture of metamorphic hydrothermal fluids with minor magmatic-derived components, which indicates the Zaozigou gold deposit can best be classified as an orogenic gold deposit.

4. Conclusion

Certain quantities of scheelite are firstly reported from the Zaozigou gold deposit in West Qinling Orogen. Scheelite is closely related to gold mineralization. It shows homogeneous CL images, MREE-enriched chondrite-normalized REE patterns, positive Eu anomalies, $3Ca^{2+} = 2REE^{3+} + \square Ca$ substitution, and distinct Sr and Mo contents. Moreover, plots

Table 1. Compilation of trace element composition of scheelite from the Zaozigou gold deposit by laser ablation ICP-MS.

Spot No.	SCH-01	SCH-02	SCH-03	SCH-04	SCH-05	SCH-06	SCH-07	SCH-08	SCH-09	SCH-10
Na	833.03	697.52	756.97	819.51	734.52	746.92	715.16	570.73	560.31	519.34
As	6.05	5.24	5.29	6.41	5.10	5.32	5.55	4.17	4.15	5.30
Sr	26.44	0.08	0.08	0.10	27.87	0.60	0.38	0.16	0.12	0.27
Y	111.17	40.31	4.75	12.96	69.51	74.55	74.99	110.39	258.18	175.92
Nb	0.53	0.45	0.50	0.51	0.43	0.33	0.42	0.41	0.61	0.44
Mo	0.26	0.20	0.29	0.24	0.24	0.25	0.23	0.17	0.19	0.19
La	37.95	16.52	12.06	10.31	20.99	14.83	18.13	14.49	3.67	10.90
Ce	67.27	26.35	12.82	15.77	49.29	35.63	43.56	39.32	37.85	60.60
Pr	8.21	2.99	1.15	2.21	6.33	4.85	5.96	7.52	15.68	18.69
Nd	35.06	12.57	3.65	10.92	24.22	20.91	24.73	46.93	161.90	154.67
Sm	11.75	4.08	0.65	3.88	5.92	6.49	6.98	23.68	152.40	97.22
Eu	53.71	18.70	3.84	8.42	18.96	16.02	17.70	37.40	110.52	69.53
Gd	14.34	4.91	0.55	4.18	6.58	7.66	8.02	30.47	224.15	124.48
Tb	2.47	0.85	0.07	0.71	1.28	1.53	1.52	5.34	38.71	21.01
Dy	14.37	4.69	0.41	3.67	8.31	9.64	9.81	28.04	181.52	101.48
Ho	2.41	0.81	0.07	0.57	1.64	1.80	1.89	4.41	24.47	14.35
Er	5.54	1.79	0.13	1.04	4.18	4.24	4.80	8.49	36.92	22.70
Tm	0.65	0.22	0.02	0.09	0.52	0.53	0.62	0.86	2.50	1.63
Yb	3.63	1.25	0.11	0.37	2.68	2.67	3.13	4.10	7.22	5.18
Lu	0.35	0.12	0.01	0.03	0.24	0.24	0.30	0.39	0.47	0.37
∑REE	368.88	136.15	40.29	75.14	220.65	201.59	222.14	361.84	1256.16	878.73
LREE	213.95	81.21	34.17	51.51	125.71	98.73	117.06	169.34	482.02	411.61
HREE	154.93	54.94	6.12	23.63	94.94	102.86	105.08	192.50	774.14	467.12
LREE/HREE	1.38	1.48	5.59	2.18	1.32	0.96	1.11	0.88	0.62	0.88
δEu	12.64	12.76	19.12	6.36	9.25	6.94	7.21	4.26	1.83	1.93

of Eu_N *vs* Eu_N^* and δEu *vs* Mo indicate a reduced fluid. Synthesis of geochemical data of scheelite more likely suggests that the Zaozigou gold deposit is derived from metamorphic hydrothermal fluids and classified as an orogenic gold deposit. In conclusion, the geochemistry of scheelite provides critical information on hydrothermal systems, highlighting its great potential to reveal ore-fluid physicochemical conditions, origin of mineralizing fluids and ore genesis.

CRediT authorship contribution statement

Jia-jun Liu conceived of the presented idea. Meng-xu Guo, De-gao Zhai and Jia-jun Liu performed the computations and verified the analytical methods. Jia-jun Liu encouraged Meng-xu Guo and Rui Zhu to investigate the Zaozigou gold deposit. All authors discussed the results and contributed to the final manuscript.

Acknowledgment

This work was supported by Records of China’s Mineral Geology from the China Geological Survey (DD20190379), the State Key Program of National Natural Science Foundation of China (41730426), and the 111 Project of the Ministry of Science and Technology (BP0719021).